

The impact of the modified Poisson–Boltzmann model on protein bound to a lipid coated silicon nanowire field effect transistor biosensor in an electrolyte environment

Umapathi Krishnamoorthy, Meenakshi Sundaram Nachiappan & Kalpana Palanisamy

To cite this article: Umapathi Krishnamoorthy, Meenakshi Sundaram Nachiappan & Kalpana Palanisamy (2018): The impact of the modified Poisson–Boltzmann model on protein bound to a lipid coated silicon nanowire field effect transistor biosensor in an electrolyte environment, Physics and Chemistry of Liquids, DOI: [10.1080/00319104.2018.1464162](https://doi.org/10.1080/00319104.2018.1464162)

To link to this article: <https://doi.org/10.1080/00319104.2018.1464162>



Published online: 02 May 2018.



Submit your article to this journal [↗](#)



Article views: 15



View related articles [↗](#)



View Crossmark data [↗](#)



The impact of the modified Poisson–Boltzmann model on protein bound to a lipid coated silicon nanowire field effect transistor biosensor in an electrolyte environment

Umapathi Krishnamoorthy^a, Meenakshi Sundaram Nachiappan^b and Kalpana Palanisamy^c

^aDepartment of Electrical and Electronics Engineering, Jansons Institute of Technology, Coimbatore, India;

^bDepartment of Physics, Government Arts College for women, Tirupur, India; ^cDepartment of Electronics and Communication Engineering, PSG College of Technology, Coimbatore, India

ABSTRACT

The aim of this work was to analyse the electrostatic potential profile, various effects of electrolyte concentrations, and the influences of surface charge on a protein bound to a lipid coated Silicon nanowire field effect transistor (Si-NW FET) biosensor by implementing the modified Poisson–Boltzmann (MPB) model. In this work, we modelled a lipid monolayer-coated Si-NW FET for the sensing of proteins, which consisted of variable amounts of aspartic acid. The electrostatic potential profile, protein charge distributions, the response to various electrolyte concentration, and the impacts of various surface charge were studied by implementing the MPB model with the Si-NW FET biosensor. Additionally, a comparison between the use of the MPB and the Poisson–Boltzmann model in studying the effects of various surface charges was carried out. Taken together, it was found that the MPB model showed a higher resolution in studying the Si-NW FET biosensor model when higher concentrations and surface charges were administered.

ARTICLE HISTORY

Received 9 November 2017
Accepted 8 April 2018

KEYWORDS

Lipid coated NWFET; biosensor modelling; protein sensing; MPB modelling

1. Introduction

The importance and the use of nanostructures in the sensing of biological and chemical materials has been a growing area of research, with the previously successful use of biomaterials in combination with one-dimensional (1D) nanostructures [1]. The use of 1D nanostructures in nanowire fabrication and the important device applications has been established [2]. Specifically, the use of nanowires in field effect transistors (FETs) for applications in both chemical and biological sensors has been shown [3, 4]. Additionally, the sensitivity of a nanowire FET and the electrochemical detection of a nanowire FET has also been determined [5, 6]. Most recently, there has been the development of the Schottky barrier nanowire FET model for specific applications in liquid environments [7, 8].

Various enzyme monolayer-functionalized FET biosensors have been classified and analysed using real-time quantitative methods [9]. Additionally, the detection of peptides with a single charge has been achieved, and it is now possible to differentiate single charge variations on analytes, even in physiological electrolyte solutions [10]. Furthermore, in the literature the incorporation of various lipid membranes and supported lipid monolayers and bilayers into semiconductor devices has been achieved [11].

Previously, modelling of the distribution of charges of artificial proteins such as the aspartic acid and the green fluorescent protein has been successfully shown [12]. Therefore, in this work we have

modelled the distribution of charges from artificial proteins on a lipid coated nanowire FET in an electrolyte environment.

In electrolyte environments, the Poisson–Boltzmann (PB) model is only sensible if the applied electric field is reasonably small and it considers ions as point like charge. [13,14,15,16,17]. Additionally, the utilisation of the PB model is not possible in systems with high ionic concentrations or in systems with highly applied electric fields [16]. Therefore, due to the number of limitations of the PB equation on solid-liquid interfaces, for a more accurate determination of steric effects on aqueous solutions, the modified Poisson–Boltzmann (MPB) model developed by Borukhov *et al.* is used [14,15,16,17]. The MPB model takes into account the steric effects of the ions, which considers the finite volume of the ions. The modern MPB theory commonly used in electrolyte environments can be defined as,

$$-\epsilon \nabla^2 \psi(r) = -z e c_i^\infty \frac{2 \sinh\left(\frac{z_i e \psi(r)}{2kT}\right)}{1 + 2\nu \sinh^2\left(\frac{z_i e \psi(r)}{2kT}\right)} \quad (1)$$

In equation (1), $\psi(r)$ is the electric potential forces that act on each ion, c_i^∞ is the bulk concentration of the ion ' i ', z_i is the valence number of the ion, e is the proton charge (1.6×10^{-19} C), T is the temperature ($^\circ\text{K}$), k is the Boltzmann constant (1.38×10^{-23} J/ $^\circ\text{K}$), and $\epsilon = \epsilon_0 \epsilon_r$, where ϵ_r is the relative permittivity of the solution and ϵ_0 is the dielectric constant of the vacuum. In this work, the relative permittivity for water, silicon (Si), and silicon dioxide (SiO_2) used were 80, 12.1, and 4.2, respectively. Additionally, the total volume fraction of the positive and negative ions, also known as the packing parameter, $\nu = (z + 1)a^3 c_i^\infty$, where a is the effective ion size.

By including the effective ion size a in the MPB equation, the steric effects of the ion are incorporated and make clear the resolution needed in designing the biosensor. By reducing the finite volume ion size a to zero in these equations, it changes the equation to the standard PB equation and allows it to be used in understanding point-like charges without the steric impacts. Furthermore, the molar ionic concentrations M_i are expressed as $M_i = c_i^\infty 10^{-3}/N_A$, where N_A is the Avogadro constant (6.022×10^{23}).

In electrolyte environments of higher concentrations, the MPB equation has been shown to be more useful than the PB equation [15, 16]. Previously, the MPB equation has been implemented and used successfully in higher surface charges and concentrations [18]. Furthermore, an initial implementation of the use of the MPB equation in nanowire FET with various finite size ions in electrolyte environments has been studied [19].

Therefore, in order to further investigate the effects of the MPB model in a nanowire FET biosensor, we have modelled artificial proteins bound to a lipid monolayer-coated silicon nanowire (Si-NW) FET biosensor and the electrostatic potential distributions, protein charge distributions, various electrolyte concentration effects and various surface charges impacts have been analysed in varying electrolyte environments. Also, the results of this work have been compared to results using the PB model, to further interrogate the various effects that surface charge has on the system.

2. Methods

2.1 The lipid coated silicon nanowire FET model

To analyse the electrostatic potential profile as well as the effects of electrolyte concentration and surface charges on the specific protein charge distributions, we subjected our lipid coated Si-NW FET to a liquid environment and implemented the MPB equation model. A schematic of the lipid coated Si-NW FET in both three-dimensional (3D) and two-dimensional (2D) is shown in Figure 1 (a) and (b), respectively, with the channel length of the semiconducting Si nanowire 1000 nm, the diameter 20 nm, and the length of the source and drain contacts 100 nm.

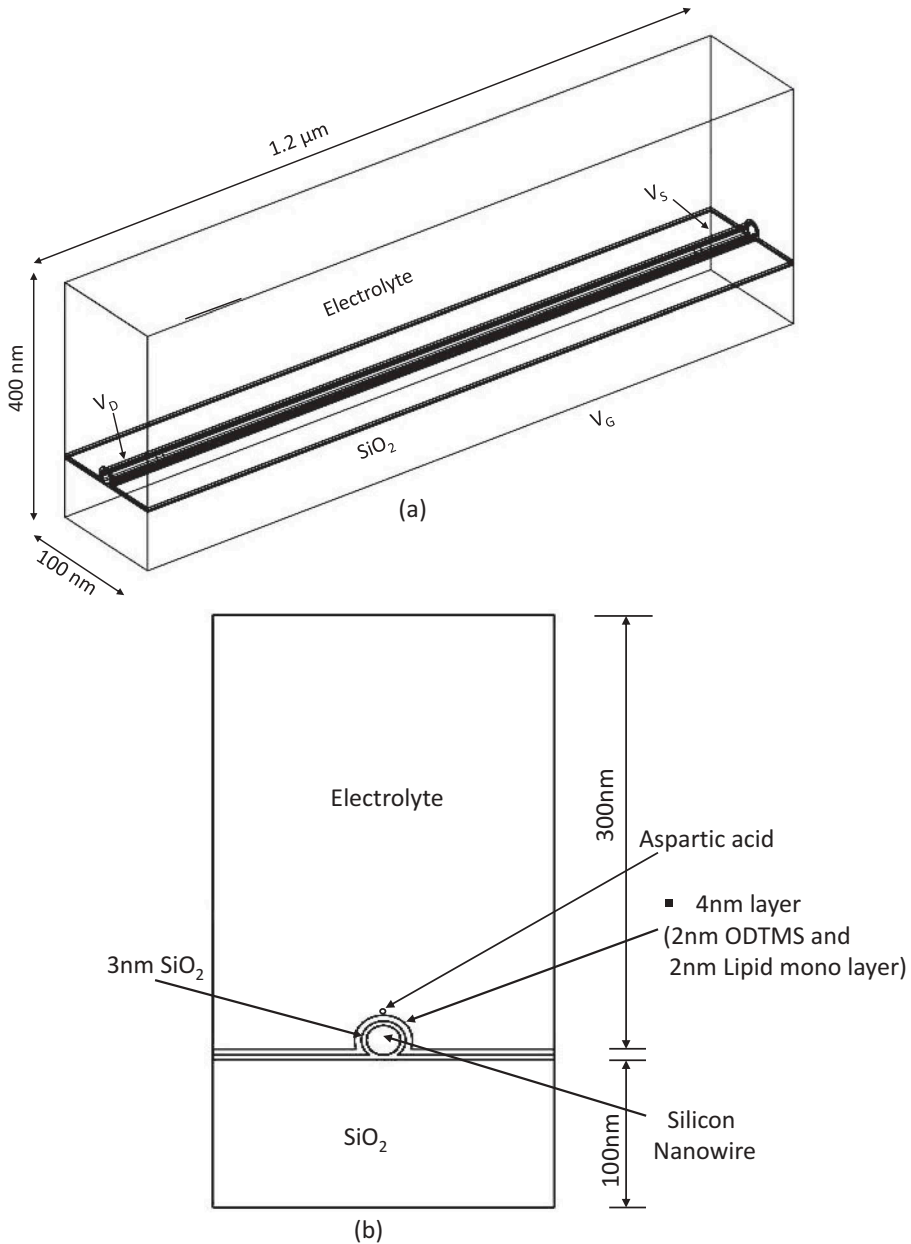


Figure 1. Schematic representations as both (a) 3D and (b) 2D images of the lipid-coated Si-NW FET model.

A SiO_2 native oxide layer (3 nm) enclosed the entire nanowire surface. To make the Si nanowire bio-functionalised and to passivate the SiO_2 oxide layer, a 2 nm monolayer of ODTMS (octadecyltrimethoxysilane) was used. The dielectric constant of the ODTMS layer was defined as $\epsilon_r = 1.5$ and the assumption that there is no interface charge between the ODTMS and oxide surface due to the passivation layer was made. The ODTMS layer was surface-functionalised with a lipid membrane that allowed the specific binding of molecules. In this study, a 2 nm lipid monolayer consisting of DOGS-NTA (1, 2-dioleoyl-*sn*-glycero-3- $\{[N(5\text{-amino-1-carboxypentyl})\text{iminodiacetic acid}]\text{succinyl}\}$) incorporated into two matrix lipids (DMPC (1,2-dimyristoyl-*sn*-glycero-3-phosphocholine) and cholesterol) was used as

the lipid membrane, with the knowledge that the use of a lipid monolayer determined experimentally [10] and the model has been previously examined [12]. Additionally, due to the insulating property of the lipid membrane, the same parameters of ODTMS were considered. Furthermore, since the lipid monolayer was noted as very dense, no electrolytes were considered in this region. For simplicity in this analysis, only a 4 nm layer was considered, since it has the same dielectric constant $\epsilon_r = 1.5$, for both 2 nm of ODTMS and the 2 nm lipid monolayer. Also, a 1.2 nm diameter of aspartic acid protein was bonded to the top of the lipid monolayer. We also applied a drain-source voltage of $V_{ds} = 0.5$ V and a gate-source voltage of $V_g = 5$ V.

In this study, we implemented the PB model and MPB model in a potassium chloride (KCl) electrolyte environment to determine the electrostatic potential profile, protein charge distribution, effects of various concentrations, and the influences of surface charge on the Si-NW FET biosensor model. Additionally, after modelling and the setting the parameters of the device geometry, the PB and MPB equations were solved numerically using COMSOL finite element analysis software.

2.2 Modelling of the protein charge distribution

The focus of this study was the binding of the negatively charged aspartic acid to the lipid monolayer. The use of biotin-streptavidin is not considered appropriate in this work due to the known high affinity binding between biotin and avidin, whereas the use of [(N-(5-amino-1-carboxypentyl) iminodiacetic acid) succinyl] (NTA) is much more advantageous due to the lipid headgroup binding and the easily reversible immobilisation. In addition, the chelating of lipids with histidine-tagged (His-tag) proteins and peptides and their subsequent fusion to a membrane has been previously established [20]. When divalent nickel ions (Ni^{2+}) are bound to the NTA headgroups that comprise the lipid monolayer, this creates surface functionalisation that permits the coupling of His-tagged proteins or peptides to the membrane [20].

It is well established that artificial protein structures where amino acids have been labelled with a His-tag have the ability to bind to the NTA headgroup of the lipid monolayer. This histidine backbone is known to be negatively charged, due to the aspartic acid that carry one negative charge each for the binding to the tag. Therefore, it is possible to produce hexahistidine-labelled (His6) peptides with a variable number of attached charged residues. The charge of the aspartic acids has been altered between taking a single charge (His6Asp1) and up to ten charges (His6Asp10). For each charge, the variable signal can be distinguished and peptides with higher charges will result in an increased sensor reaction.

Modelling of aspartic acid volume charge can be calculated as follows [12]:

$$\text{Volume charge} = -z \times e \times \sigma_{NTA}/1.2 \text{ nm} \quad (2)$$

Where $\sigma_{NTA} = f_{NTA}/A_{NTA} = 7.7 \times 10^{12} \text{ cm}^{-2}$, f_{NTA} is surface density of the DOGS-NTA lipids (5%), A_{NTA} is the approximated headgroup area (0.65 nm^2), e is the electron charge density, z is the number of charges per peptide molecule ($z = 1, 2, 3, 4, 5$) and the diameter of the protein is 1.2 nm.

The integrated charge density of the protein region of the biosensor changes the magnitudes of $-e \sigma_{NTA}$ by increasing the number charges (z) of the aspartic acid units. In this equation, by changing the z values from 0 to 5 the volume charge is also changed. Therefore, to simplify the modelling, the aspartic acid residues were considered to be directly bound the lipid-coated Si-NW FET without any neutral part of the his-tag and from this the charge density of the protein was assumed the same as the calculated volume charges.

3. Results and discussion

3.1 Electrostatic potential distribution in the Si-NW FET biosensor coated with a lipid monolayer

For the investigation into the electrostatic potential profiles, we placed the biosensor model into an electrolyte environment of KCl at both 100 mM and 1 M concentrations, and the MPB model is applied only to the KCl electrolyte concentration area. Additionally, we have taken the effective ion size of K as 1.25×10^{-10} m and this is the value used in equation (1). Initially, the device model was tested in ‘neutral’ conditions of air without any ionic concentration and the distribution of various electric potentials along the Si-NW channel into different gate voltages can be seen in Figure 2 (a) and 2 (b), where the applied gate voltages were from -10 V to 10 V at both $V_d = 0.5$ V and $V_d = 0$ V, respectively. It was noted that due to the change of gate voltages the electric potential for the Si-NW channel dropped. Following on from this, the electric potential profile along the Si-NW axis for both 100mM and 1M KCl was examined (Figure 2 (c)). As can be seen, if the ionic concentration level increases as to does the electric potential drop. Taken together, when there were no ions, the difference in electric potential within the Si-NW was found to be higher, while it got smaller with increasing ionic concentrations due to the screening effect.

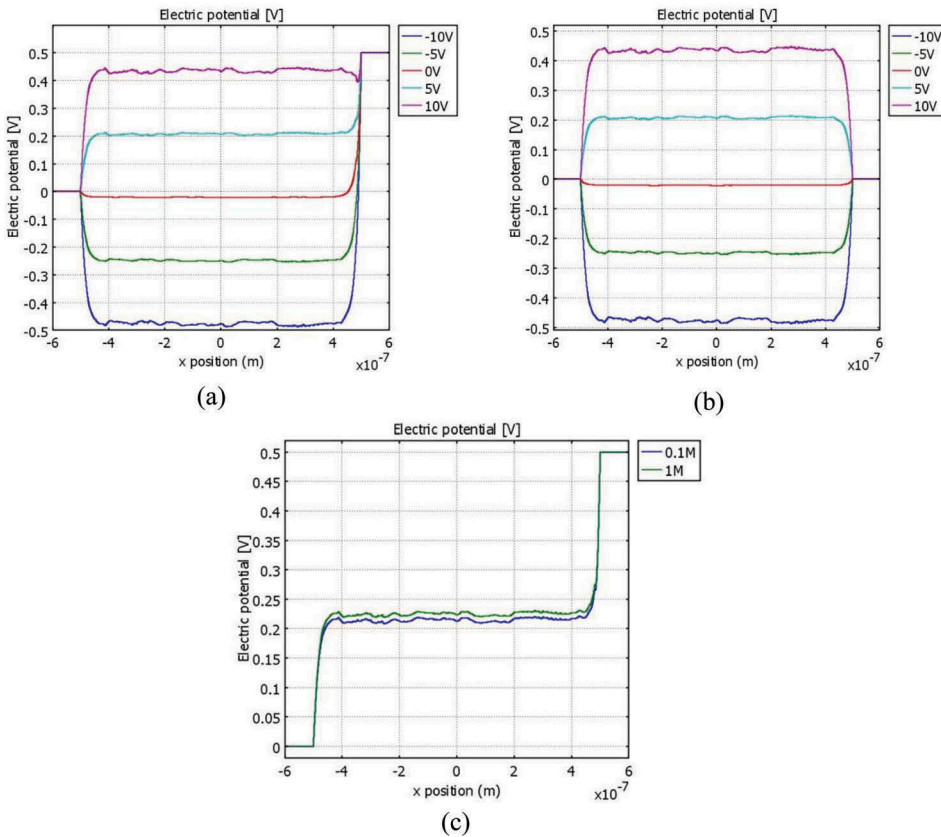


Figure 2. One dimensional electrostatic potential along the nanowire axis in air environment **(a)** $V_d = 0.5$ V, with the gate voltages -10 V to 10 V. **(b)** $V_d = 0$ V, with the gate voltages -10 V to 10 V. **(c)** Si-NW FET electric potential for 0.1 M and 1 M KCl, where the source drain voltage was $V_d = 0.5$ V and the gate voltage was $V_g = 5$ V.

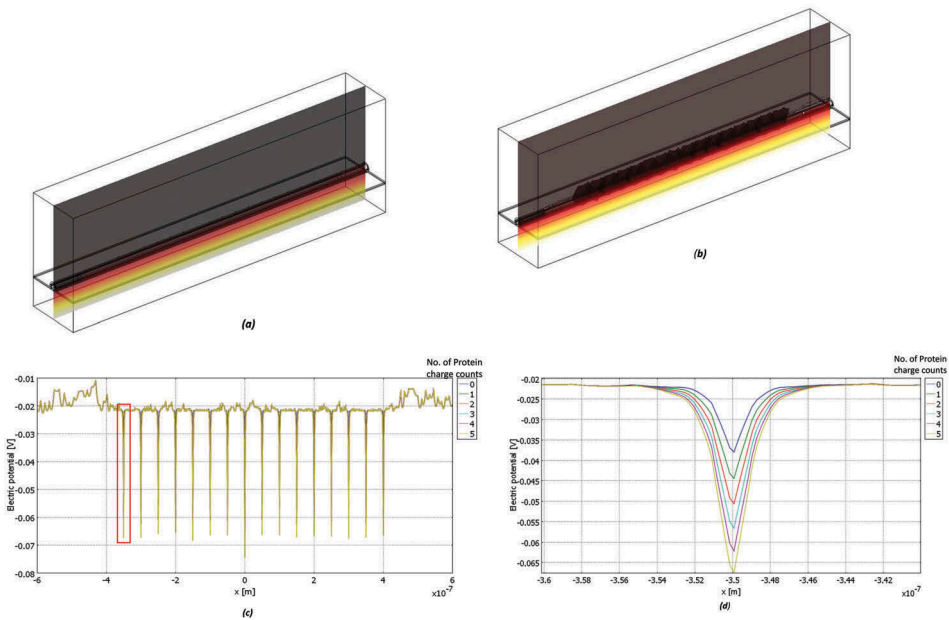


Figure 3. Protein charge distribution analysis in 3D model along the nanowire axis (a) Zero protein charge. (b) 5 aspartic acid protein charge counts. (c) Electrostatic potential characteristics due to the protein charge distribution along the nanowire axis. (d) An enlarged view of a particular area of the electrostatic potential characteristics (red box (c)).

3.2 Protein charge distributions in the Si-NW FET biosensor

To further understand the influence of the varying protein charge distribution over the Si-NW FET, we modelled and placed 16 different protein charges with a distance of 5 nm from each other on top of the lipid monolayer and the volume charge density of the individual protein was calculated using equation (2). Therefore, we increased the charge density calculated by changing the z value from 0 to 5. In Figure 3, a 3D view of the Si-NW FET protein charges distribution with both zero protein charges (a) and 5 aspartic acid charges (b) can be seen. Additionally, as noted in Figure 3 (c) the electric potential profile

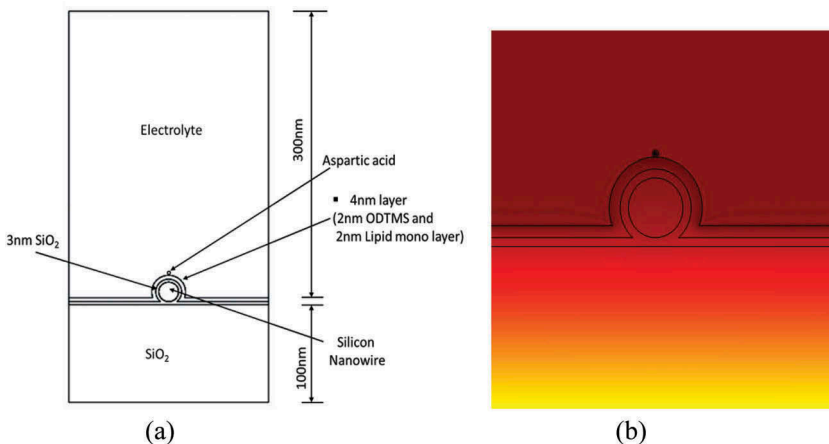


Figure 4. The effect of various concentration of electrolyte solution (KCl) on the aspartic acid charged Si-NW FET biosensor model. (a) 2 D model of Nanowire FET. (b) Surface view of the applied concentration.

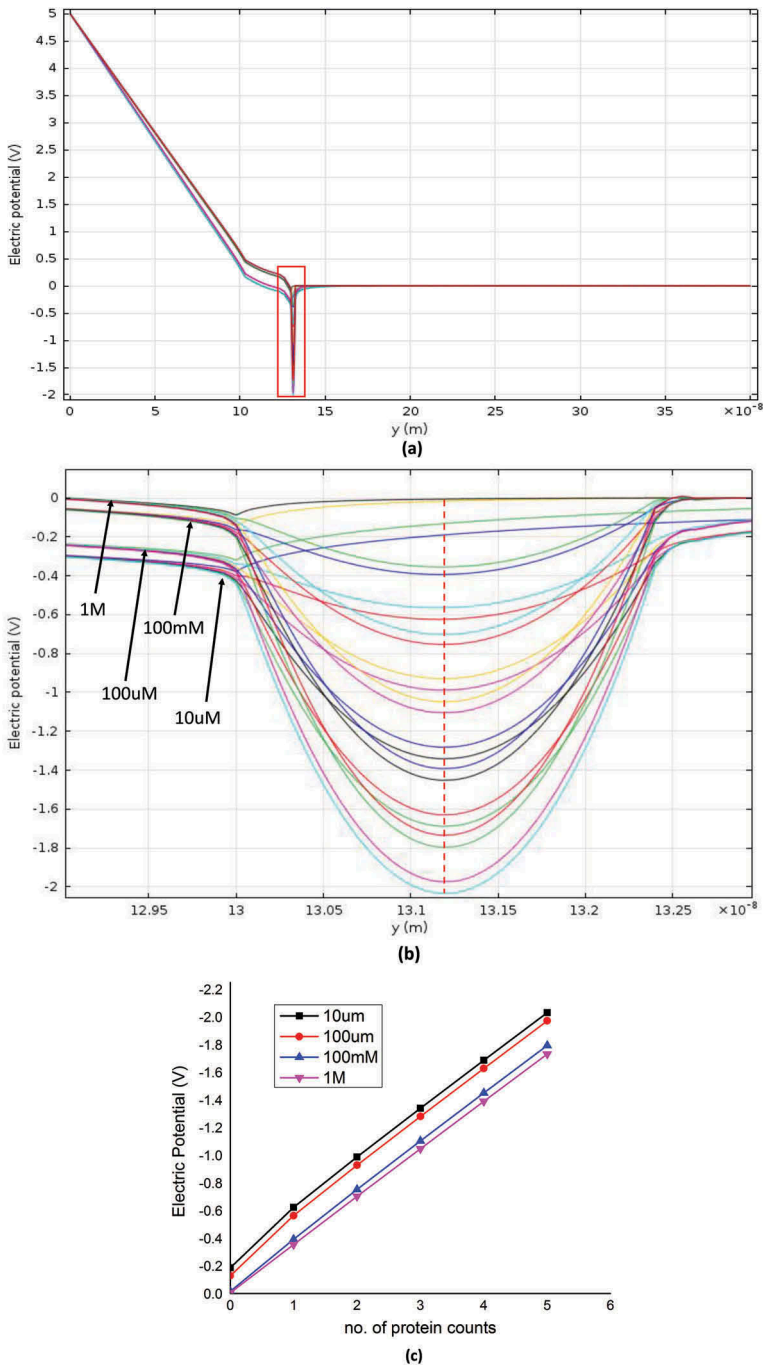


Figure 5. Electric potential difference in various KCl concentrations with increasing aspartic acid charged counts (a) Effects of various concentrations on the biosensor model. (b) An enlarged view of the highlighted (red box) area of effects of various concentrations on the biosensor model. (c) The differences in the electric potential for the same protein charge distribution for the various electrolyte concentrations. In fig (b) Red dashed line shows the measured point on the electric potential.

due to this protein charge distribution along the length of the Si-NW axis was measured. Furthermore, when a particular region of the measurement is enlarged, it is clear to see that by increasing the protein charge distribution, the electric potential drop also increased (Figure 3 (d)).

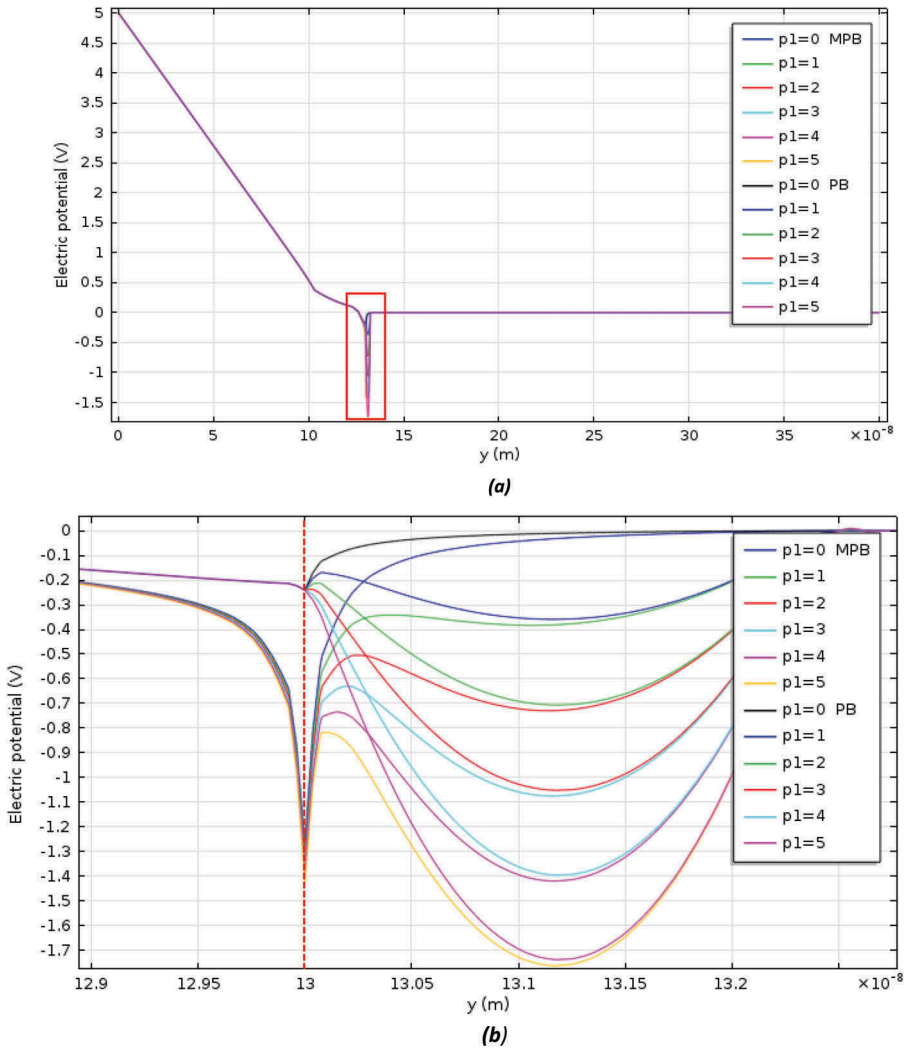


Figure 6. (a)MPB and PB model comparison with increasing aspartic acid protein charge counts with the surface charge density -0.4 C/m^2 and 1 M KCl. (b)An enlarged view of the highlighted (red box) from the comparison between the MPB and PB models.

3.3 Various electrolyte concentration effects on the Si-NW FET biosensor using the MPB model

In the study of the effects of various electrolyte concentrations including 10 μM , 100 μM , 100 mM, and 1 M KCl, on the Si-NW FET biosensor model, we considered the 2D model of the Si-NW FET, with aspartic acid model charges as shown in Figure 4. Since it is a MPB model applied only for the KCl electrolyte concentration, we considered the effective ion size of K^+ as 1.25×10^{-10} m.

As seen in Figure 5, differences between the electric potential due to the increase in the amount of charge on the aspartic acid model protein is seen with each ionic concentration, 10 μM , 100 μM , 100 mM, and 1 M. In the lower concentrations of KCl, the electric potential was found to be higher and as the concentration level of KCl increased the electric potential reduced. From this, we can see that in low ionic concentrations the Si-NW FET biosensor model is having a high

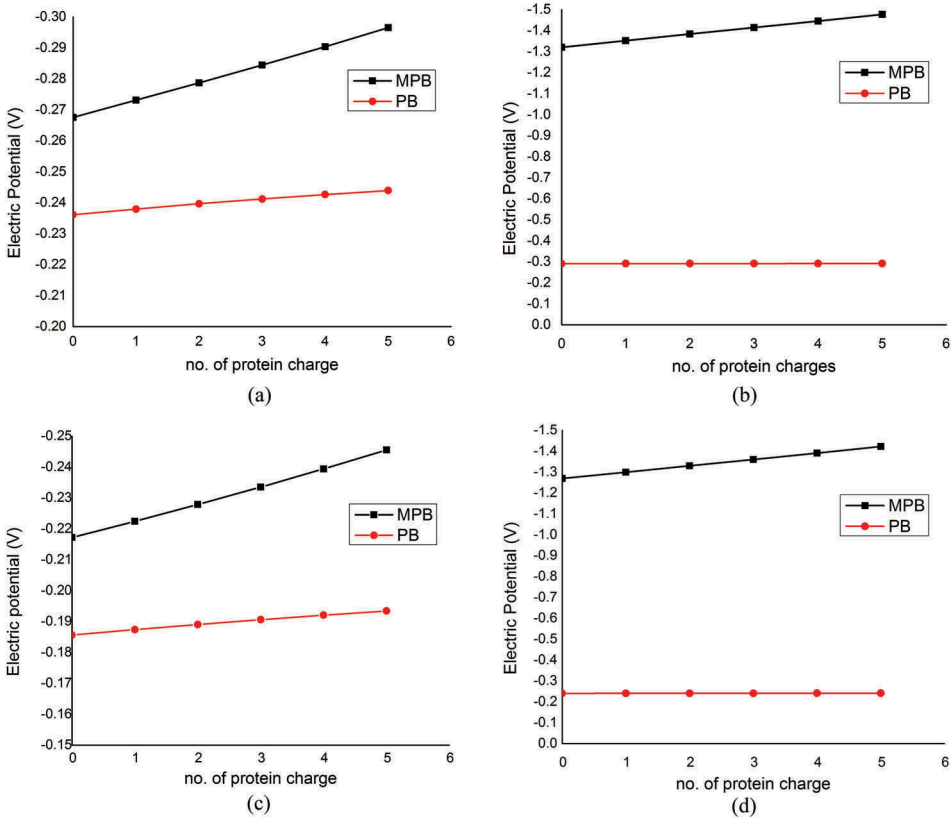


Figure 7. Electrostatic potential difference between the MPB and PB model comparisons with increasing aspartic acid charge counts with surface charge density of -0.1 C/m^2 (a, c) and -0.4 C/m^2 (b, d) and 140 mM (a, b) and 1 M KCl (c, d) concentration.

sensitivity to the external protein model charge, with this influence of the model charge on the electric potential, reduced in higher electrolyte concentrations.

3. 4 Comparison between the MPB and PB models, with various surface charges effects, in the Si-NW FET biosensor

In order to understand the effects of various surface charges on the Si-NW FET biosensor, we exposed our model to various surface charges from -0.1 to -0.4 C/m^2 and various electrolyte concentrations 140 mM and 1 M KCl while increasing the aspartic acid charge distribution from 0 to 5, in the MPB model. The comparison between MPB and PB models (full size measurement and an enlarged region (red box)) for the electrostatic potential profiles of the surface charge density -0.4 C/m^2 , 1 M KCl and increasing aspartic acid counts 1 to 5 is seen in Figure 6.

As seen in Figure 7, where the electrostatic potential profiles of the varying surface charges and varying KCl concentrations can be seen, the lower concentration produces a higher electrostatic potential for both models. Additionally, it was found that when the concentration increases the electrostatic potential decreases. This provides insight into the higher resolution achieved in using the MPB model compared to the PB model.

4. Conclusions

In this work, we have modelled the lipid-coated Si-NW FET bound with an artificial protein consisting of a number of aspartic acid charges in a KCl electrolyte environment, with the implementation of the MPB model. A number of facets of this model were studied, including a comparison between air and the electrolyte environment, the protein charges distribution while increasing the aspartic acids counts on the lipid monolayer coated Si-NW FET, and the changes to the electrostatic potential profile with various KCl concentrations. Additionally, the understanding of the effect of various surface charges in various electrolyte environments was developed with the implementation of both the MPB and the PB models. From this work it can be concluded that the MPB model provides a higher resolution to the given surface charges and concentrations in the Si-NW FET biosensor model.

Acknowledgements

The authors wish to acknowledge the facilities and support provided by the Management of PSG College of Technology, Coimbatore, India.

Disclosure statement

No potential conflict of interest was reported by the authors.

References

- [1] Cui Y, Wei Q, Park H, et al. Nanowire nanosensors for highly sensitive and selective detection of biological and chemical species. *Science*. 2001;293(5533):1289–1292.
- [2] Mikolajick T, Heinzig A, Jens Trommer, Sebastian Pregl, Matthias Grube, Gianauelio Cuniberti and Walter M. Weber. Silicon nanowires – a versatile technology platform. *Physica Status Solidi (RRL) Rapid Res Lett*. 2013;7(10):793–799.
- [3] Chen K-I, Bor-Ran L, Chena Y-T. Silicon nanowire field-effect transistor-based biosensors for biomedical diagnosis and cellular recording investigation. *Nano Today*. 2011;6:131–154.
- [4] Stern E, Wanger R, Sigworth F, et al. Importance of the debye screening length on Nanowire Field Effect Transistor sensors. *Nano Lett*. 2007;7(3405).
- [5] Griehaber D, MacKenzie R, Voros R, et al. Electrochemical biosensors— *sensor principles and architectures*. *Sensors*. 2008;8:1400.
- [6] Curreli M, Zhang R, Ishikawa FN, et al. Real-time, label-free detection of biological entities using nanowire-based FETs. *IEEE Trans Nanotechnol*. 2008;7(6):651–667.
- [7] Nozaki D, Kunstmann J, Zorgiebel F, et al. Multiscale modeling of nanowire-based Schottky-barrier field-effect transistors for sensor applications'. *Nanotechnology*. 2011;22.
- [8] Nozaki D, Kunstmann J, Zorgiebel F, et al. Ionic effect on the transport characteristics of nanowire-based FETs in liquid environment'. *Nano Res*. 2014;7:380.
- [9] Kharitonov AB, Zayats M, Lichtenstein A, et al. Enzyme monolayer-functionalized field-effect transistors for biosensor applications. *Sensors & Actuators B*. 2000;70:222.
- [10] Lud SQ, Nikolaides MG, Haase I, et al. Field effect of screened charges: electrical detection of peptides and proteins by a thin-film resistor. *Chem Phys Chem*. 2006;7(2):379–384.
- [11] Kataoka-Hamai C, Miyahara: Y. Field-effect detection using phospholipid Membranes. *Sci Technol Advan Mat*. 2010;11(3):033001.
- [12] Birner S, Uhl C, Bayer M, et al. Theoretical model for the detection of charged proteins with a silicon-on-insulator sensor. *J Physics: Conf Ser*. 2008;107(01).
- [13] Lee J, Shin M, Ahn C-G, et al. "Effects of pH and ion concentration in a phosphate buffer solution on the sensitivity of silicon nanowire bioFETs". *J Korean Phys Soc*. 2009;55:1621–1625.
- [14] Borukhov I, Andelman D, Orland H. Steric effects in electrolytes: a modified Poisson-Boltzmann equation. *PhysRev Lett*. 1997;79:435–438.
- [15] Kilic MS, Bazant MZ, Ajdari A. Steric effects in the dynamics of electrolytes at large applied voltages. I. Double-layer charging. *Phys Rev E*. 2007;75:021502.
- [16] Pham P, Howorth M, Planat-Chretien A, et al.: 'Numerical simulation of the electrical double layer based on the poisson-boltzmann models for ac electro osmosis flows', COMSOL Users Conference, 2007

- [17] Hamou RF, Biedermann PU, Erbe A, et al. Numerical simulation of probing the electric double layer by scanning electrochemical potential microscopy. *Electrochimica Acta*. 2010;55:5210.
- [18] Lou P, Lee JY. Ionic size effect on the double layer properties: a modified poisson boltzmann theory. *Bull. Korean Chem Soc*. 2010;9:2553.
- [19] Krishnamoorthy U, Nachiappan MS, Palanisamy K. Investigation of the effect of finite-sized ions on the nanowire field-effect transistor in electrolyte concentration using a modified poisson-boltzmann model. *Phys Chem Liquids*. 2017;56(2):231-240.
- [20] Schmitt L, Dietrich C, Tampe R. Synthesis and characterization of chelator-lipids for reversible immobilization of engineered proteins at self-assembled lipid interfaces. *J Am Chem Soc*. 1994;116:8485.